

Collective dynamics in a model of sliding charge-density waves. II. Finite-size effects

Christopher R. Myers* and James P. Sethna

Laboratory of Atomic and Solid State Physics, Cornell University, Ithaca, New York 14853-2501

(Received 25 June 1992; revised manuscript received 2 November 1992)

The unusual finite-size effects exhibited by a class of models of sliding charge-density-wave (CDW) conductors are examined within the context of an automaton model we have developed which allows us to probe close to threshold in large systems. We demonstrate the existence of two distinct parts of the finite-size regime, and describe the nature of each subregime. We present evidence for unusual finite-size scaling, whereby finite-size effects are not simply driven by the divergence of the velocity-velocity correlation length ξ . Finally, we compare simulations of sliding CDW's with experimental data to suggest that finite-size effects may be present in real CDW conductors.

I. INTRODUCTION

The depinning of a charge-density-wave (CDW) system in an applied dc field is a dynamic critical phenomenon, which has been studied previously by other authors¹ as well as in a companion paper (part I) preceding this paper.² The purpose of this paper is to examine the prominent and somewhat unusual finite-size effects observed in simulations of the model introduced and studied in part I. Finite-size effects in sliding CDW's are of interest for several reasons. First, the circumstances of the finite-size crossover and the nature of the finite-size regime are somewhat atypical for systems near a second-order phase transition. Second, because the finite-size regime above threshold is unusually large, the critical scaling regime is rather small. As a result, the theoretical—and probably the experimental—determination of the scaling exponents describing the transition has been considerably hampered for several years. Third, recent experimental measurements^{3,4} reveal that the underlying phase-coherent domains in certain samples are considerably larger than had once been thought; this implies that some experimental systems should show considerable finite-size effects due to the critical growth of dynamic correlations.

Finite-size effects in simulations of a critical system are typically viewed as an artifact of the process of simulation, although useful information about the critical properties of the system can often be extracted via the techniques of finite-size scaling. A finite-size crossover typically occurs when the diverging correlation length ξ becomes of order the system size L . Estimates of the intrinsic correlation length exponent ν can be made from measurements of a finite-size scaling correlation length exponent ν_{fs} . If the finite-size effects are driven simply by the divergence of the intrinsic correlation length ξ , the two exponents are equal: $\nu_{fs} = \nu$. In most thermodynamic critical systems, a finite-size system does not exhibit a sharp transition; rather, the transition is rounded near the critical point on the scale of the finite-size regime.

The finite-size effects in sliding CDW's are rather different. While sharp estimates of the finite-size scaling correlation length exponent ν_{fs} are difficult to achieve, it is clear that the finite-size effects are not simply driven by the growth of the correlation length ξ , since the two scal-

ing exponents differ: $\nu_{fs} \neq \nu$. Furthermore, the velocity-velocity correlation length ξ is considerably smaller than the system size L at the onset of finite-size effects, suggesting that some other mechanism (e.g., the presence of a second diverging length scale) governs the finite-size crossover. In addition, the depinning transition [within the class of Fukuyama-Lee-Rice⁵ (FLR) models] is sharp even in systems of finite size. And finally, the finite-size regime does not consist simply of the "single-particle" limit that was originally conjectured but rather has a rich structure of its own.

In this paper, we study finite-size effects within the context of the automaton model introduced and examined in our preceding paper (part I) on the critical phenomena of depinning.² We refer readers to the preceding paper for complete details of the model, but note here that our automaton is intended as a caricature of the lattice FLR model⁶ which describes the dynamics of the CDW phase ϕ_i at each site on a d -dimensional cubic lattice:

$$\dot{\phi}_i = -\frac{\delta H}{\delta \phi_i} = F + J \Delta_i^2(\phi) - V \sin[2\pi(\phi_i - \beta_i)], \quad (1)$$

where

$$\Delta_i^2(\phi) = \sum_{\langle j \rangle} (\phi_j - \phi_i) \quad (2)$$

is the finite-difference curvature (lattice Laplacian) of the phase field ϕ at site i , the sum being over nearest neighbors $\langle j \rangle$ to site i ; F is proportional to the applied electric field; V is the strength of the pinning potential; J is the elastic coupling strength (with appropriate scaling to make the elastic constants isotropic); and β_i are drawn uniformly from the interval $[0,1)$. Our automaton model is particularly well suited to the task of studying finite-size effects, since we need to probe close to threshold in large systems in order to undertake such a study. In the conventional lattice FLR model (1), approaching threshold in large systems is difficult because of the critical slowing down associated with motion through "sticking points." Since our model bypasses the slow motion through sticking points by projecting forward in time to the hopping motion of unstable phases,² it does not slow

down near threshold. And since we incorporate a time lag to mimic motion through a sticking point, our model possesses the same single-particle scaling behavior close to threshold in a finite system, namely, that associated with the saddle-node bifurcation of a single mode.

In Sec. II, we begin by providing a qualitative overview of the dynamics of a sliding CDW in a finite system to elucidate the types of possible behavior. We also introduce velocity data from simulations of various system sizes to highlight some of the major points we wish to make in this paper. We then present a more detailed investigation of the finite-size regime, focusing on the two subregions which comprise it: the “single-particle regime” characterized by the existence of one sliding domain and a CDW velocity v which scales with reduced field f roughly as $v \sim f^{1/2}$, and a “few-particle sparse regime” where there is more than one sliding domain and a general flattening in $v(f)$ although there is no simple scaling of velocity with reduced field. In Sec. III, we compare results from simulations with experimental data on an extremely good sample of NbSe₃ to suggest that finite-size effects of the type reported here are present in some experimental CDW conductors.

II. FINITE-SIZE EFFECTS IN SIMULATIONS

A. Overview of the sliding state in finite systems

The power-law scaling of the CDW velocity v with reduced driving field f which was studied in the previous paper occupies only a small interval in f even in systems of rather large size. Figure 1, a log-log plot of the average CDW velocity v as a function of the reduced driving field $f \equiv (F - F_T)/F_T$ in two dimensions for systems of size 256^2 , demonstrates a wealth of other behavior. We demarcate four regions, and describe the two finite-size regions (I and II) below.

Just above threshold (region I, the single-particle finite-size regime), the CDW dynamics is dominated by a single site, the “threshold site,” which is critical at the depinning threshold. The threshold site dominates the dynamics in this regime both spatially and temporally. If we start from the pinned threshold state and increase the field slightly so as to depin the CDW, the threshold site is initially the only unstable phase, and all other phases must wait for the threshold site to depin and trigger a pulse which destabilizes the rest of the system. In this single-particle regime, there is only one such pulse or “sliding domain” characterizing the motion of the CDW. Since the velocity-velocity correlation length ξ represents the average size of the sliding domains, in this regime $\xi \approx L$. By shading the hopping times in the manner introduced in the preceding paper, we demonstrate the character of this single domain, in Fig. 2.

The temporal dominance of the threshold site is reflected in the fact that the velocity v scales roughly with reduced field f in the manner $v \sim f^{1/2}$. This is because almost the entire period T is consumed with the slow motion of the threshold site through its sticking point. For very small reduced fields, the duration of the pulse triggered by the depinning of the threshold site is much

shorter than the sticking time of the threshold site itself. The pulse propagation time also is not nearly so sensitive to small changes in f , since the remaining sites in the system are not particularly close to their local thresholds. The square-root scaling of v with f reflects the saddle-node bifurcation of the threshold site at the critical point. As f increases, $v(f)$ can begin to flatten, since the sticking time of the threshold site ceases to dominate the pulse propagation time. Even if the velocity begins to flatten and ceases to scale with a square-root power law, as long as there is some time in the cycle when the threshold site is the only active site, there will be only one sliding domain and the threshold site will control the dynamics.

As the field is increased further, eventually the privileged position occupied by the threshold site becomes undermined. This signals the onset of region II. In any number of fashions, the CDW can reorder its sliding sequence and develop new sliding domains. In some samples (realizations of the random pinning phases $\{\beta\}$), this may happen if the field is increased enough to destabilize a second site in the system; that is, a second site may be able to depin without having to wait for the depinning pulse initiated by the threshold site to sweep across the system. In other samples, the sticking time for

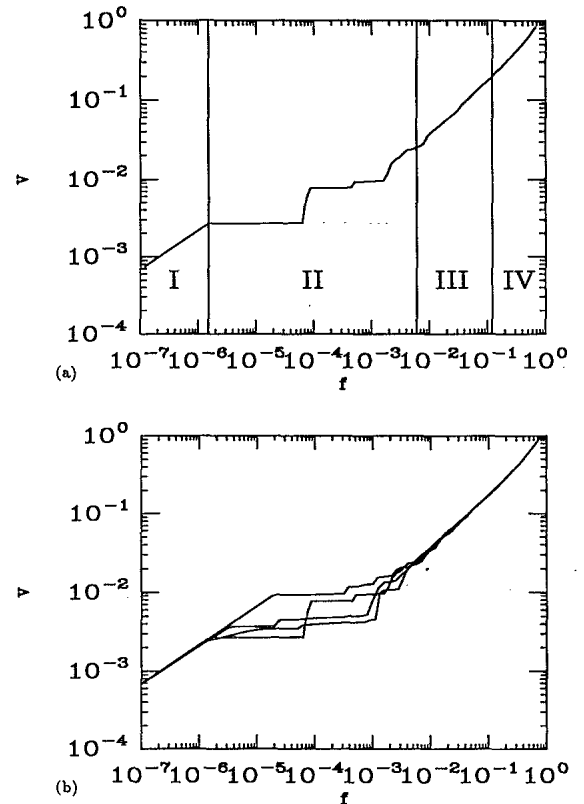


FIG. 1. CDW velocity v as a function of reduced field f , in (a) a single two-dimensional sample of size 256^2 and (b) several two-dimensional samples of size 256^2 . We demarcate four velocity regimes: the “single-particle regime” (I), the “few-particle sparse regime” (II), the “critical regime” (III), and the “high-field crossover regime” (IV). In an infinite system, only regions III and IV persist.

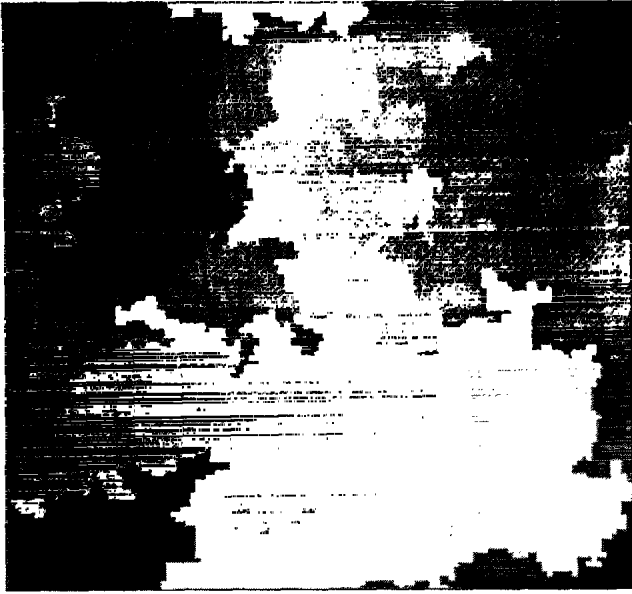


FIG. 2. Hopping times for the periodic orbit executed by a two-dimensional CDW of size 128^2 , for $f=10^{-7}$. Each site is shaded according to its hopping time: black denotes hopping early in the cycle, while white denotes hopping late. The cycle has been arbitrarily initialized with the hopping of the threshold site (near the lower-left corner). The orbit is periodic, so black and white are identified in this shading scheme. There is only one “sliding domain” at this field, encompassing the entire system. Therefore, in this regime, $\xi=L$.

the threshold site may become short enough that it hops again before the initial pulse has passed through the whole system. In any case, once multiple sliding domains form, the period T can drop dramatically since pulses need not travel so far to depin stable sites. This process leads to sharp jumps in the velocity, as are evident in Fig. 1. As mentioned in the preceding paper, as f is increased sufficiently further, the number of sliding domains becomes large enough (in the critical regime) that the evolution of v with f becomes smooth.

B. CDW velocity in systems of various sizes

In this section we demonstrate several features of the behavior of CDW systems of finite size, the most important being the existence of more than one diverging length scale as the threshold is approached from above. Because of this, the onset of finite-size effects scales in a manner differently than one would expect based on the intrinsic velocity-velocity correlation length ν , and the standard techniques of finite-size scaling collapses are not particularly useful.

We begin by presenting data of the type shown in Fig. 1, in $d=1, 2$, and 3 , for a variety of system sizes. In Fig. 3, we show data in $d=1$ for several samples each of linear size L ranging from 256 to 8192; Fig. 4 shows several samples in $d=2$ with L ranging from 8 to 256; and Fig. 5 shows data in $d=3$ for L ranging from 8 to 45.

There are several things to glean from these three sets

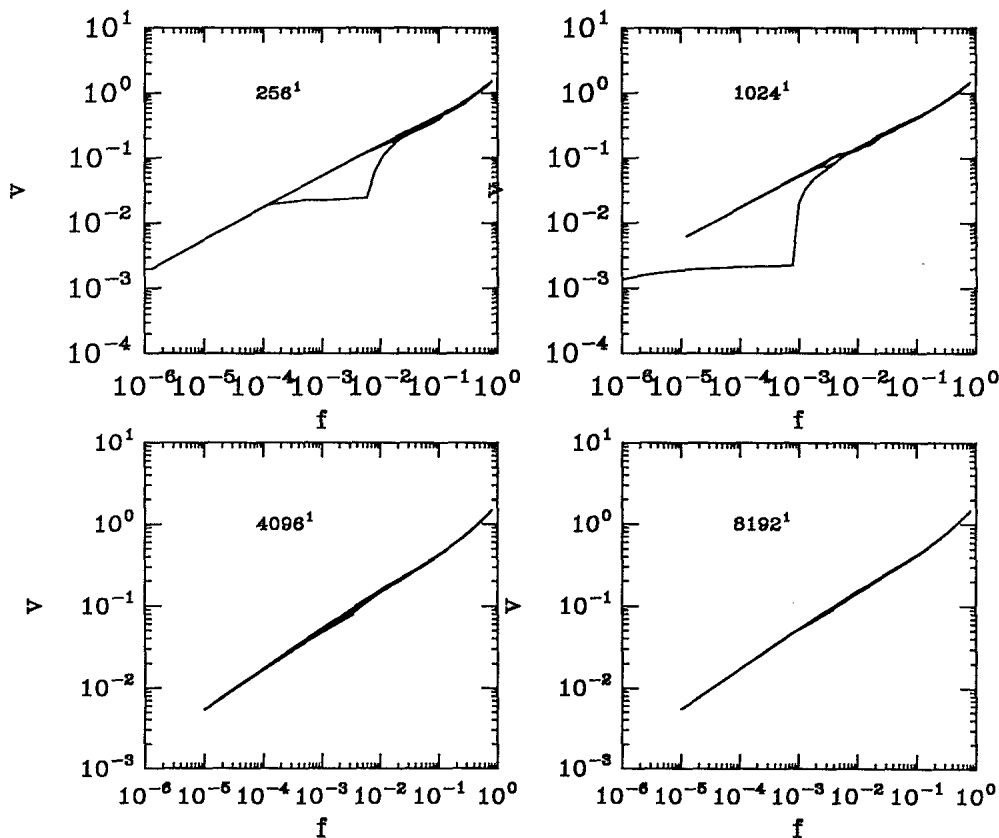


FIG. 3. Velocity data for various sample sizes in $d=1$, to illustrate finite-size effects.

of figures. First, note that the extent in $\log_{10}(f)$ of the intermediate few-particle sparse regime (region II) grows with the system size L . Although they are not completely well defined, we can roughly identify two finite-size crossovers: the “outer” finite-size crossover separating regions II and III, and the “inner” finite-size crossover separating regions I and II. The width in $\log_{10}(f)$ grows with system size because the inner crossover moves to smaller f with increasing L faster than the outer crossover does. If we denote the inner crossover as occurring at a reduced field f_{fs}^i , and the outer as occurring at a field f_{fs}^o , then we can define two finite-size scaling correlation length exponents, ν_{fs}^i and ν_{fs}^o :

$$f_{fs}^i \sim L^{-1/\nu_{fs}^i}, \tag{3}$$

$$f_{fs}^o \sim L^{-1/\nu_{fs}^o}. \tag{4}$$

The growth in the width of the intermediate finite-size regime with L derives from the fact that $\nu_{fs}^i < \nu_{fs}^o$. We demonstrate this in Fig. 6, where we plot, in $d=2$ and 3, the crossover points f_{fs}^i and f_{fs}^o as a function of L . From these data, we estimate the finite-size exponents to be $\nu_{fs}^i = 0.4 \pm 0.1, 0.3 \pm 0.1$ in $d=2$ and 3, respectively, and $\nu_{fs}^o = 0.8 \pm 0.2, 0.6 \pm 0.2$. It should also be noted that both sets of exponents are probably unequal to the values for the intrinsic correlation length exponent ν presented in part I, namely, $\nu=0.5$ in both $d=2$ and 3. The errors are such that we cannot say with certainty that $\nu \neq \nu_{fs}^i$ and $\nu \neq \nu_{fs}^o$, but it appears that this is the case.

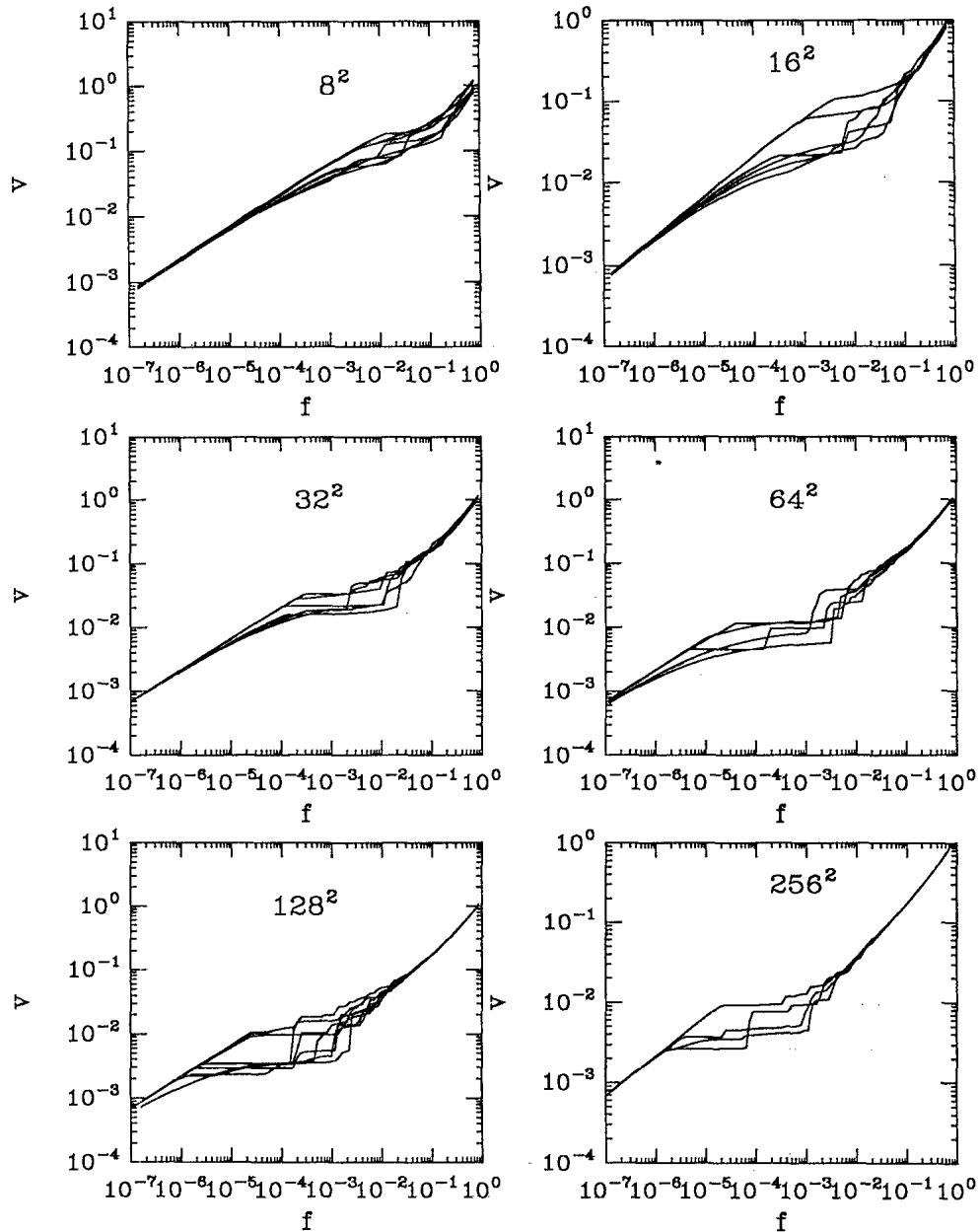


FIG. 4. Velocity data for various sample sizes in $d=2$, to illustrate finite-size effects.

Because there is more than one such scaling exponent, it is immediately clear that a typical finite-size scaling approach cannot collapse velocity data from different system sizes onto a single scaling curve. Finite-size scaling can only translate data on a log-log plot, but it cannot stretch such data. At best, we can try to align different data sets at individual points to get separate estimates of the finite-size exponents ν_{fs}^i and ν_{fs}^o .

One should also note that there is considerable sample-to-sample variation in $\log_{10}(v)$ within the finite-size regime for a given size L and dimension d . This variation appears to be greatest in $d=2$, where there is a tendency for individual $v(f)$ curves to cluster into a high-velocity branch and a low-velocity branch; this is most evident for the particular samples shown of size 16^2 and 128^2 . Associated with this variation is the fact that the sample-to-sample fluctuations in $\log_{10}(v)$ within the finite-size regime tend to grow rather than diminish with system size, as the high-velocity and low-velocity branches spread apart. In $d=1$, most curves tend to lie on the high-velocity branch; indeed, the data presented for systems of size 4096^1 and 8192^1 do not show any curves on the low-velocity branch. In $d=3$, on the other hand, most samples tend to lie on the low-velocity branch, as is particularly evident in the data for 32^3 . We shall address these sample-to-sample variations and the dimensional trends below in Sec. II C.

C. Velocity fluctuations in the finite-size regime

Although the absolute sample-to-sample finite-size fluctuations in v vanish in the thermodynamic limit, the fluctuations in $\log_{10}(v)$ tend to grow with increasing system size. We can understand these fluctuations in part via the concept of the reactivation time, which we can define unambiguously in the single-particle regime. The reactivation time t_r is the amount of time required for the threshold site to be “reactivated”² (returned to a condition of instability) after having previously hopped:

$$t_r \equiv T - \tau_{\text{thr}}, \quad (5)$$

where T is the full period of the CDW orbit and τ_{thr} is the sticking time of the threshold site. We have studied the distribution of reactivation times $D(t_r)$ for various samples as a function of system size L at a fixed reduced field f . We plot $D(t_r)$ in $d=2$ and 3 for various system sizes, in Figs. 7 and 8, respectively. We find that there are two pieces which make up this distribution, one peaked at short times and one peaked at long times. The short-time piece does not shift with system size, but the long-time piece moves out to longer times as L increases. These two pieces appear to be associated with two topologically distinct reactivation pulses. The first, a local reactivation pulse, involves only sites in the neighborhood of the threshold site, and therefore does not depend on system

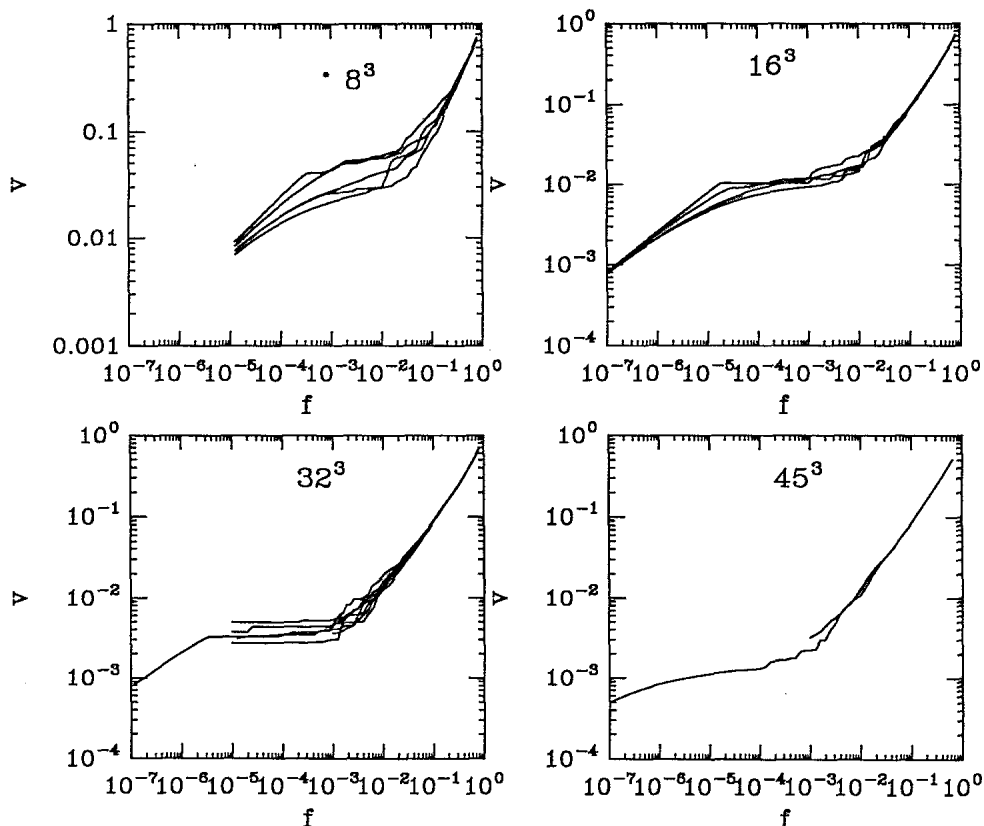


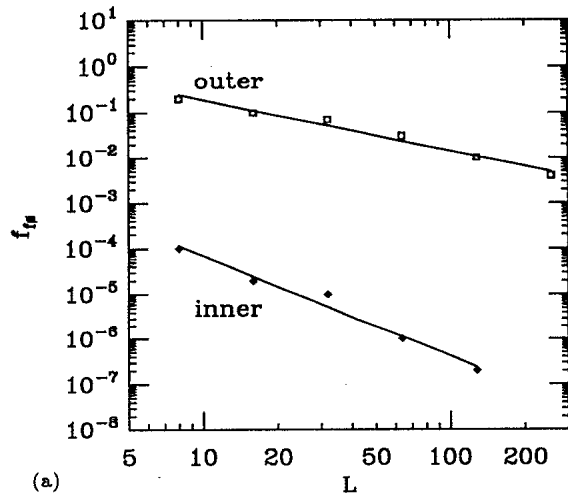
FIG. 5. Velocity data for various sample sizes in $d=3$, to illustrate finite-size effects.

size. The second, a nonlocal reactivation process, must wrap around the boundary and reactivate the periodic image of the threshold site. Since the distance to the periodic image grows with L , so does the time for such a reactivation to occur. The high-velocity branch in the $v(f)$ curves appears to be associated with sites which reactivate locally in a short time, while the low-velocity branch arises from the nonlocal processes which take longer.

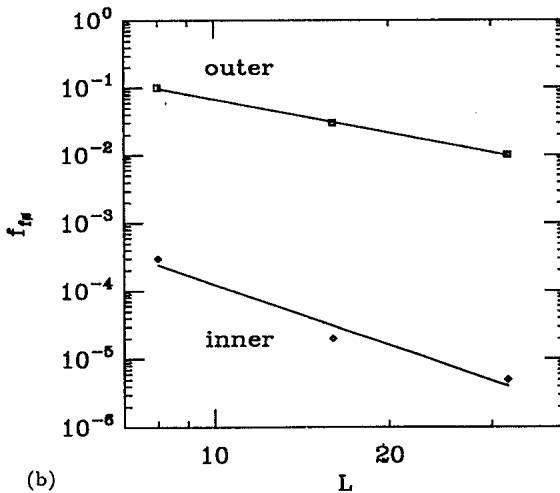
Comparison of the reactivation time distributions in $d=2$ and 3, however, reveals that the relative weight of the two processes is quite different in each dimension. The two pieces carry roughly equal weight in $d=2$, while in $d=3$ almost all reactivations are of the long-time, nonlocal type. In $d=1$ (not shown), almost all reactivations are concentrated in the local, short-time piece. This dimensional dependence is reminiscent of the return statistics for random walks: return to the origin is common in $d=1$, marginal in $d=2$ and unlikely in $d \geq 3$. If we consider the reactivation path as being something akin to a

random walk, then it follows that as d increases, the chance of locally reactivating the threshold site (without having to resort to the periodic boundary conditions to return to the origin) will decrease.

Because of this tendency for almost all reactivations in $d=1$ to be local and those in $d=3$ to be nonlocal, the typical velocity fluctuations are greatest in $d=2$, where local and nonlocal reactivations occur with roughly equal probability. A set of velocity curves for various samples in $d=3$ does not typically exhibit large fluctuations in



(a)



(b)

FIG. 6. Inner and outer finite-size crossover points (f_{is}^i and f_{is}^o , respectively) as a function of system size L , in $d=2$ (a) and 3 (b). We extract from these data the scaling exponents ν_{is}^i and ν_{is}^o . A power-law fit to the data gives rise to the solid lines of slope $-1/\nu_{is}^i$ and $-1/\nu_{is}^o$.

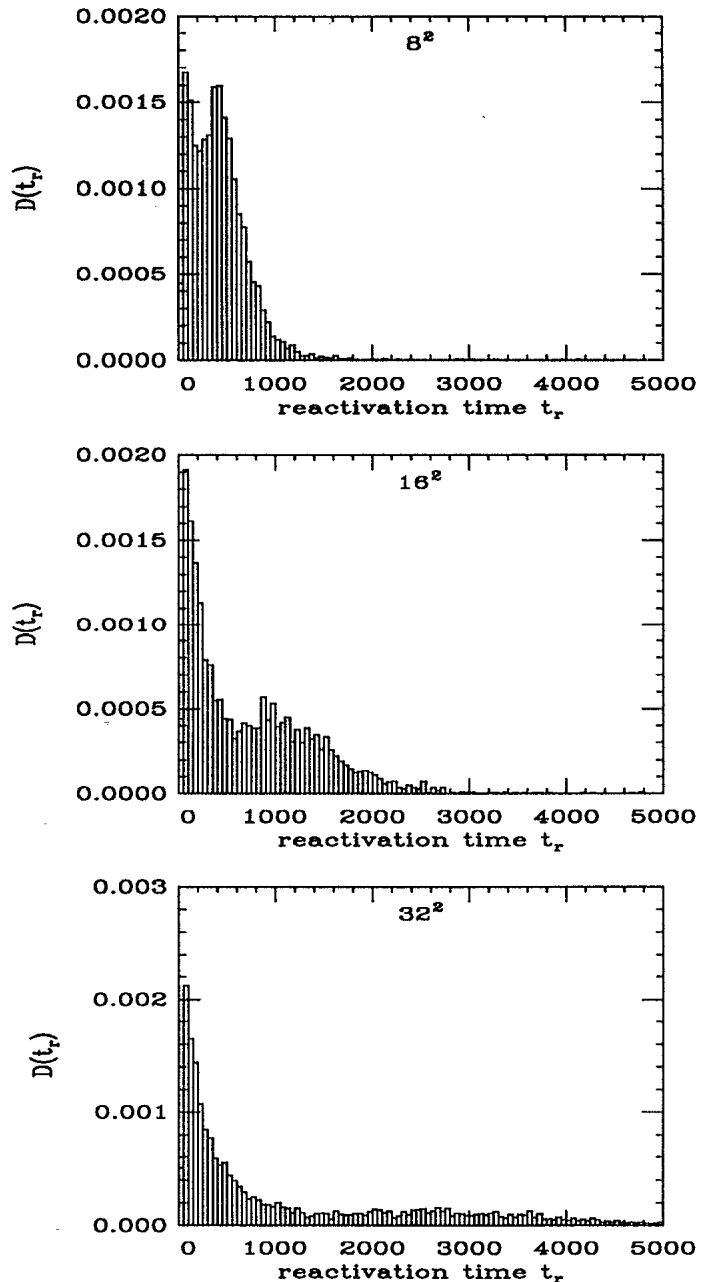


FIG. 7. Reactivation time distributions $D(t_r)$ for various system sizes L , in $d=2$, at a reduced field $f=10^{-7}$ defined for each sample. Note the existence of a short-time piece of the distribution which does not shift with system size, and a long-time piece which moves out to longer times with increasing L .

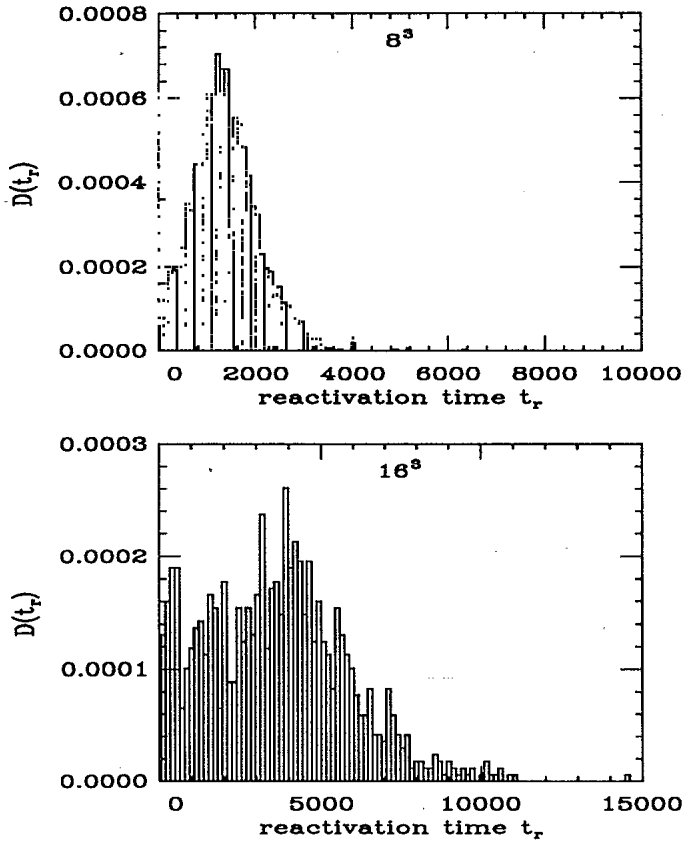


FIG. 8. Reactivation time distributions $D(t_r)$ for various system sizes L , in $d=3$, at a reduced field $f=10^{-7}$ defined for each sample. Note that most of the weight is in the long-time peak, unlike in $d=2$.

$\log_{10}(v)$, as is evident in Fig. 5. This is because very few samples belong to the shorter-time (higher-velocity branch).

Although the arguments presented above are only directly pertinent to the single-particle regime, where the period decomposes simply into threshold-active and threshold-inactive pieces, the growth in the relative velocity fluctuations and the dimensional tendencies described seem to hold in the intermediate few-particle regime, suggesting that the basic process described contributes to at least part of the dynamics at those fields.

D. Unusual finite-size effects above threshold

Prior to our simulations and those by Middleton on the lattice FLR model for small system sizes,⁷ it had been conjectured^{8,9} that (1) finite-size effects will become evident when the correlation length becomes of order the system size, $\xi \approx L$, and (2) the system will crossover from the critical scaling regime (region III) to the single-particle finite-size regime (region I), with $v \sim f^{1/2}$. Simulations of both the lattice FLR model and our automaton model demonstrate the existence of the intermediate few-particle finite-size regime. Furthermore, Middleton⁷ has explained the existence of the intermediate finite-size regime in mean-field theory.

As alluded to previously, we have found several anomalous finite-size effects in sliding CDW's. First, the system deviates from the critical scaling regime and begins to show finite-size effects when the correlation length ξ is still considerably smaller than the system size L , suggesting that something other than the simple growth of the correlation length governs the finite-size crossover. Second, the scaling of the finite-size crossover with system size, as embodied in the exponent ν_{fs}^0 , is inconsistent with the divergence of the correlation length, as described by the exponent ν ; i.e., $\nu_{fs}^0 \neq \nu$. Third, the finite-size onset is not just a simple crossover from the critical regime to the single-particle regime, but involves the intermediate sparse regime.

An exact determination of the crossover from critical scaling is difficult. One reason is that the critical regime is small or even nonexistent (in smaller systems), making it difficult to pinpoint where critical scaling ends and finite-size effects begin. A second reason is that the non-self-averaging nature of the finite-size regime must be accounted for: some samples continue to exhibit apparent power-law scaling to lower fields than do other samples of the same size. As a result, we feel it is generally better to examine $v(f)$ curves for many samples of a given system size to estimate the onset of the finite-size regime, rather than average the velocity from many samples. The considerable error in the estimates of ν_{fs}^0 reported above reflect this difficulty.

Further evidence that the finite-size crossover is not governed simply by the divergence of the velocity-velocity correlation length ξ is the fact that ξ is considerably smaller than the system size L at the crossover. We demonstrate this in Fig. 9, where we shade the hopping times in a system of size 128^2 at a field of $f=0.005$, the approximate crossover point in a system of this size. The domain structure apparent from this shading scheme reflects the spatial extent of dynamic correlations. In a conventional critical system, we would see finite-size effects when $\xi \approx L$; in the CDW this would imply that there is a single sliding domain characterizing the motion. Figure 9 demonstrates that there are many such domains at the finite-size crossover. We find that $\xi \sim f^{-\nu}$ in the critical regime, and that as f is lowered, ξ continues to grow, although in a nonscaling manner, until the system crosses over at very small f into the single-particle regime. It is only within the single-particle regime that $\xi=L$.

It has been noted previously that the correlation length exponent ν is "small." In particular, Sibani and Littlewood⁹ noted that the velocity-velocity correlation length exponent ν is less than $2/d$, which is expected as a lower bound for finite-size scaling correlation length exponents in certain types of disordered systems.¹⁰ This led them to suggest that there could be a second diverging length scale near threshold. Middleton^{11,7} has noted that one can define a finite-size scaling correlation length exponent ν_{fs} which does satisfy $\nu_{fs} \geq 2/d$ in $d=1$ and 2 , by considering the fluctuations in the threshold field F_T as a function of system size L . This $2/d$ scaling of threshold field fluctuations has been confirmed by the renormalization-group calculation of Narayan and Fisher.¹² Middleton

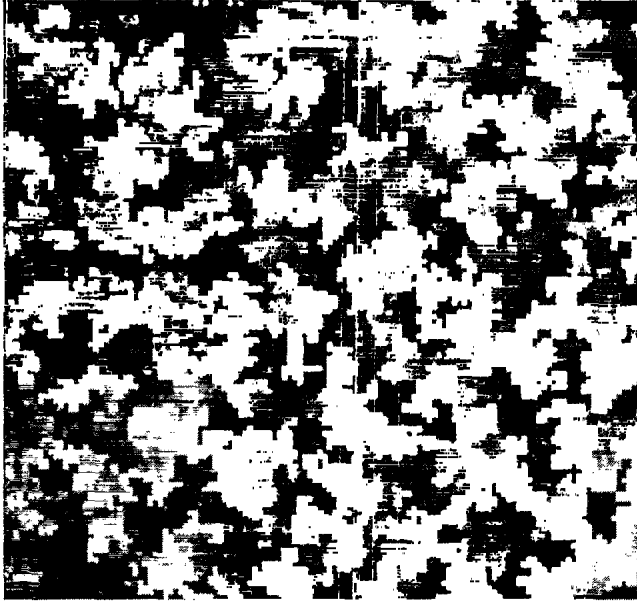


FIG. 9. Hopping times for the periodic orbit executed by a two-dimensional CDW of size 128^2 , for $f=0.005$, near the outer finite-size crossover f_{fs}^o . Each site is shaded according to its hopping time: black denotes hopping early in the cycle, while white denotes hopping late. The cycle has been arbitrarily initialized with the hopping of the threshold site (near the lower-left corner). The orbit is periodic, so black and white are identified in this shading scheme. The velocity correlation length ξ is the average size of the correlated sliding domains. Note that $\xi \ll L$ at this crossover point, in contrast to the usual scenario for finite-size effects.

has hypothesized that the finite-size fluctuations in the threshold field also govern the finite-size deviations from power-law velocity scaling above threshold. In $d=2$, he has measured $v_{fs}^o = 1.0 \pm 0.2$ for the lattice FLR model, which is not inconsistent with our rather uncertain estimate of v_{fs}^o in $d=2$. One possible source of discrepancy between the two estimates of v_{fs}^o is the fact that Middleton computed v_{fs}^o from an average of several $v(f)$ curves, whereas we did not perform such an average. At this point there is not a clear picture as to the origin of the outer finite-size crossover. Examination of the CDW motion near the crossover does not reveal an obvious larger dynamic length scale. The $2/d$ fluctuations in threshold field identified by Middleton do not necessarily imply a similar scaling of the velocity data in finite systems. And our previously proposed crossover of time scales¹³ appears inconsistent with recent simulations on a generalized time-lag CDW automaton.¹⁴

The scaling of the inner finite-size crossover, characterized by the exponent v_{fs}^i , appears to be consistent in both two and three dimensions with the relation $v_{fs}^i = 1/d$. This relation is a result of Middleton's mean-field theory of the finite-size regime,⁷ and it also is consistent with a heuristic argument based on empirical evidence we observe from our simulations. Although different samples cross over from the single-particle to few-particle regimes via different processes, the crossover typically involves having a large enough increase in reduced field f that a

second phase becomes independently unstable. In our previous paper (part I), we presented evidence that, in our automaton model, the distribution of local curvatures is flat near threshold. It follows that the typical interval in f separating the most unstable site and the second most unstable site scales like $1/N$, where N is the total number of sites in the system. Since $N=L^d$, it follows that $v_{fs}^i \approx 1/d$.

III. EXPERIMENTAL STUDIES OF THE CRITICAL PHENOMENA OF DEPINNING

There has been considerable interest in the possibility of observing critical scaling in the depinning of experimental CDW conductors. Most effort has been devoted to determining the value of the velocity (or CDW current) exponent ζ . Unfortunately, experimentally measured values of ζ have varied even more widely than those determined via simulation. Sample quality—or more appropriately, the lack thereof—has been identified by Thorne¹⁵ as a major culprit in this uncertainty. We would like to suggest that, even in samples of extremely good quality, finite-size effects could overshadow any possible measurement of critical exponents. In an extremely good NbSe₃ sample studied by Thorne¹⁶ that exhibited a highly uniform and coherent current density, it has been estimated that $\zeta \approx 1$. Furthermore, it has been estimated that this particular sample was effectively two-dimensional since the transverse Lee-Rice length was comparable to the sample thickness. Thorne estimates¹⁷ that the sample contained on the order of 70×70 phase-coherent (“Lee-Rice”) domains. Our simulations would suggest that the critical regime in a system of this size is extremely tiny or even nonexistent, so it is likely that this estimate of $\zeta \approx 1$ reflects the near-linear dependence of the high-field crossover regime rather than the strict power-law scaling of the critical regime. One might imagine using a less pure sample with a smaller phase-coherence length in the hopes of “squeezing” more Lee-Rice domains into the sample, but typically these samples have sufficiently nonuniform current densities that they are probably unsuitable for studies of critical phenomena.

The rather small effective size of high-quality samples, e.g., the 70×70 Lee-Rice domains quoted above, suggests that finite-size effects may play an important role in these samples. Indeed, looking for a substantial scaling regime in a system this size is—according to our simulations—fruitless. Given that the finite-size regime in simulations is so unusually large, it makes sense to look for signatures of finite-size effects rather than power-law scaling.

Experimental studies of CDW current-voltage characteristics typically measure the differential resistance dV/dI vs V/V_T , where V is the applied voltage, V_T is the threshold voltage, and I is the total (normal + CDW) current. This differential resistance is more sensitive to subtle changes in current, particularly changes which occur over small ranges in voltage. For the high-quality sample referred to above, we have plotted dV/dI vs V/V_T in Fig. 10. We have also plotted in this figure dV/dI for one of our two-dimensional samples of size 128^2 . (A simulation of size 64^2 would obviously make a

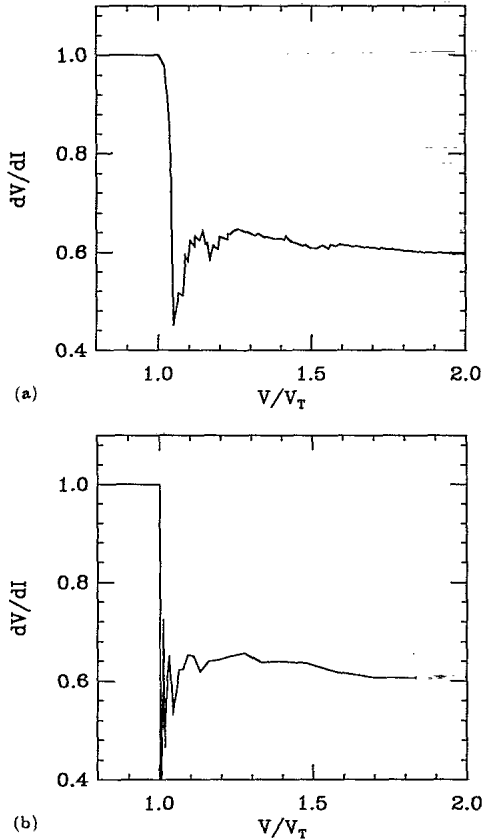


FIG. 10. Comparison of the differential resistance dV/dI for (a) an extremely high-quality sample of NbSe₃ and (b) a simulation of our automaton model in a two-dimensional system of size 128^2 .

more appropriate comparison with the 70^2 estimated size, but the dV/dI curve for such a sample would not look very different than that presented for the sample of size 128^2 .) Since our simulation measures only the CDW contribution to the current, we have added an arbitrary normal current to compare with the experimental data. The ratio of the normal to CDW conductances is a free parameter in this fit, the variation of which only alters the vertical position of dV/dI relative to the ohmic step for $V/V_T < 1$, but changes no other features in the plot.

As is seen in Fig.10, the experimental and simulated dV/dI curves are qualitatively very similar. The flat step for $V/V_T < 1$ represents the ohmic resistance of the normal carriers below threshold. Both experiment and simulation show a sharp dip just above threshold, then a rise in dV/dI for slightly larger fields, and finally a slow decrease to a saturated high-field limit. In the simulation, the origin of these features is clear. The sharp dip just above threshold corresponds to the single-particle (square-root scaling) regime; the rise in dV/dI is associated with the general flattening in the velocity which is characteristic of the few-particle sparse regime; the spikes superimposed on the bump arise from sharp jumps in the velocity which are associated with the introduction of new sliding domains; and the slow drop in dV/dI corresponds to the passage through the small critical regime

and into the high-field crossover regime.

The features observed in the experimental dV/dI curve in Fig. 10 are common to many samples, but are certainly not present in all samples. Other effects might be invoked to explain these features; macroscopic sample inhomogeneity, producing several regions of the CDW which depin at slightly different fields, could presumably give rise to a similar response. The fact that these data are from a sample which by all measures exhibits an extremely uniform and coherent current density, however, leads one to believe that the features are intrinsic to the sliding CDW itself.

Ideally, one would like to test whether or not the features described are actually due to finite-size effects. One approach would involve measuring dV/dI in a number of samples for which a reasonable estimate of the dimensionality and total domain number can be made and extracting an estimate for the scaling of the finite size regime with system size and dimensionality. Unfortunately, uneven quality from sample to sample will hamper such an investigation.

The features present in Fig. 10 are also sometimes evident near mode-locked steps in CDW's subjected to a combined ac-dc field. This serves to support the contention^{18,19,13} that the approach to a mode-locking transition is critical in the same manner as the approach to the dc depinning transition, exhibiting the same sort of growing dynamic correlations.

IV. SUMMARY AND CONCLUSIONS

We have described an intriguing set of phenomena associated with finite-size effects in sliding CDW's arising from the growth of dynamic correlations near the depinning transition. The finite-size regime is unusually prominent, becoming apparent when the velocity-velocity correlation length ξ is still rather small compared to the system size L . We have measured both the intrinsic correlation length exponent ν and the finite-size scaling correlation length exponents ν_{fs}^v and ν_{fs}^v , and have demonstrated their inequality, implying the existence of multiple length scales in the dynamics. Although we do not understand the precise reason for the premature onset of finite-size effects, we do understand its consequences. In particular, the large finite-size regime dominates the rather paltry critical scaling regime, making determination of critical exponents in simulations very difficult. The signature of these finite-size effects is present in some experimental data on sliding CDW's, which is not so surprising given the rather small effective sizes of certain samples.

The obvious unresolved question centers on the cause of the observed finite-size scaling behavior, such as the identification of a larger diverging length scale. Unusual finite-size behavior has been noted in sandpile models,²⁰ which are similar in spirit to this class of CDW models, and the resolution of this question may involve these other systems as well.

ACKNOWLEDGMENTS

We would again like to thank A. A. Middleton for many delightful conversations regarding our work and

his work. We thank R. E. Thorne for his assistance in comparing our work with his experimental data. We would also like to acknowledge useful conversations with S. N. Coppersmith, D. S. Fisher, P. B. Littlewood, O. Narayan, and S. Ramakrishna. This work was supported

by NSF Grant Nos. DMR-8451921 and DMR-9118065, and computing facilities were provided in part by the Cornell-IBM Joint Study on Computing for Scientific Research.

*Present address: Institute for Theoretical Physics, University of California, Santa Barbara, CA 93106.

- ¹D. S. Fisher, Phys. Rev. Lett. **50**, 1486 (1983); Phys. Rev. B **31**, 1396 (1985); P. B. Littlewood, *ibid.* **33**, 6694 (1986); H. Matsukawa, J. Phys. Soc. Jpn. **57**, 3463 (1988); S. N. Coppersmith and D. S. Fisher, Phys. Rev. A **38**, 6338 (1988); P. B. Littlewood and C. M. Varma, Phys. Rev. B **36**, 480 (1987); P. Sibani and P. B. Littlewood, Phys. Rev. Lett. **64**, 1305 (1990); A. A. Middleton and D. S. Fisher, *ibid.* **66**, 92 (1991); A. A. Middleton, Ph.D. thesis, Princeton University, 1990.
- ²C. R. Myers and J. P. Sethna, preceding paper, Phys. Rev. B **47**, 11 171 (1993).
- ³J. McCarten, M. Maher, T. L. Adelman, and R. E. Thorne, Phys. Rev. Lett. **63**, 2841 (1989).
- ⁴E. Sweetland, C.-Y. Tsai, B. A. Wintner, J. D. Brock, and R. E. Thorne, Phys. Rev. Lett. **65**, 3165 (1990).
- ⁵H. Fukuyama, J. Phys. Soc. Jpn. **41**, 513 (1976); **45**, 1474 (1978); H. Fukuyama and P. A. Lee, Phys. Rev. B **17**, 535 (1977); P. A. Lee and T. M. Rice, *ibid.* **19**, 3970 (1979).
- ⁶N. Teranishi and R. Kubo, J. Phys. Soc. Jpn. **47**, 720 (1979); L. Pietronero and S. Strässler, Phys. Rev. B **28**, 5863 (1983); H. Matsukawa and H. Takayama, Solid State Commun. **50**, 283

(1984); P. B. Littlewood, Phys. Rev. B **33**, 6694 (1986).

- ⁷A. A. Middleton, Ph.D. thesis, Princeton University, 1990.
- ⁸D. S. Fisher, Phys. Rev. B **31**, 1396 (1985).
- ⁹P. Sibani and P. B. Littlewood, Phys. Rev. Lett. **64**, 1305 (1990).
- ¹⁰J. T. Chayes, L. Chayes, D. S. Fisher, and T. Spencer, Phys. Rev. Lett. **57**, 2999 (1986).
- ¹¹A. A. Middleton and D. S. Fisher, Phys. Rev. Lett. **66**, 92 (1991).
- ¹²O. Narayan and D. S. Fisher, Phys. Rev. Lett. **68**, 3615 (1992); Phys. Rev. B **46**, 11 520 (1992).
- ¹³C. R. Myers, Ph.D. thesis, Cornell University, 1991.
- ¹⁴C. R. Myers (unpublished).
- ¹⁵R. E. Thorne, Bull. Am. Phys. Soc. **36**, 584 (1991).
- ¹⁶Sample no. 68 in R. E. Thorne, Ph.D. thesis, University of Illinois, 1987.
- ¹⁷R. E. Thorne (private communication).
- ¹⁸H. Matsukawa, J. Phys. Soc. Jpn. **57**, 3463 (1988).
- ¹⁹A. A. Middleton, O. Biham, P. B. Littlewood, and P. Sibani, Phys. Rev. Lett. **68**, 1586 (1992).
- ²⁰L. P. Kadanoff, S. R. Nagel, L. Wu, and S.-M. Zhou, Phys. Rev. A **39**, 6524 (1989).